Improved Quasi-Static Method with Step Doubling Time Adaptation

Zachary M. Prince*, Dr. Jean C. Ragusa*, Yaqi Wang†

*Department of Nuclear Engineering, Texas A&M University, College Station, TX
†Idaho National Laboratory, Idaho Falls, ID
zachmprince@tamu.edu, jean.ragusa@tamu.edu, yaqi.wang@inl.gov

INTRODUCTION

The imminent restart of the Transient Reactor Testing Facility (TREAT) at Idaho National Laboratory (INL) has brought significant attention to the development of transient reactor modeling. TREAT was designed to subject fuels and other reactor components to various degrees of neutron pulses, from minor transients to accident scenario. Inherently, this task requires predicting pulse responses due to various control rod movements; which is a complicated endeavor. Originally, this was done using an iterative process of rod movements and measuring the resulting response. With the advances in computer modeling, the current goal, preceding the restart, is to use simulation to characterize responses before experiments take place. However, neutron transient modeling is extremely computationally expensive due to the required implicit time-stepping. Therefore, methods that mitigate computation time, with minimal detriment to accuracy, are highly desired. This paper will describe the improved quasi-static method (IQS), which hopes to decrease computation time significantly from traditional "brute force" transient methods.

IQS is a spatial kinetics method that involves factorizing the flux solution into time-dependent amplitude and space- and time-dependent shape [1, 2]. The impetus of the method is the assumption that shape is weakly time-dependent, so expensive space-dependent evaluations are only required on large time steps. While inexpensive amplitude evaluations are performed on much smaller time steps to retain accuracy. IQS has been tested extensively on kinetics benchmarks with constant time steps. However, to test it's viability for TREAT simulations, evaluating IQS's performance with time adaptation is required. The rest of thispaper will brefly desribe the derivation of IQS, the time adaptation technique used, and results from two kinetic benchmarks.

THEORY

In this Section, we recall the equation for the IQS method, starting from the standard multi-group diffusion equations with delayed neutron precursors in operator form:

$$\frac{1}{v^g}\frac{\partial \phi^g}{\partial t} = \frac{\chi_p^g}{k_{eff}}\sum_{g'=1}^{G}(1-\beta)\nu^{g'}\Sigma_f^{g'}\phi^{g'} - \left(-\nabla\cdot D^g\nabla + \Sigma_r^g\right)\phi^g + \sum_{g'\neq g}^{G}\Sigma_s^{g'\to g}\phi^{g'} + \sum_{i=1}^{I}\chi_{d,i}^g\lambda_i C_i\,, \quad 1\le g\le G \tag{1}$$

$$\frac{dC_i}{dt} = \frac{\beta_i}{k_{eff}}\sum_{g=1}^{G}\nu^g\Sigma_f^g\phi^g - \lambda_i C_i\,, \quad 1\le i\le I \tag{2}$$

Factorization is an important step in the derivation of the IQS method. The factorization approach leads to a decomposition of the multigroup flux into the product of a time-dependent amplitude (p) and a space-/time-dependent multigroup shape (φ):

$$\phi^g(\boldsymbol{r},t) = p(t)\varphi^g(\boldsymbol{r},t) \tag{3}$$

To obtain the amplitude equations, the multigroup equations are multiplied by a weighting function, typically the initial adjoint flux (ϕ^*), and then integrated over phase-space. For brevity, the inner product over space will be represented with parenthetical notation:

$$\int_D \phi^{*g}(\boldsymbol{r})f^g(\boldsymbol{r})d^3r = (\phi^{*g}, f^g) \tag{4}$$

In order to impose uniqueness of the factorization, one requires the following:

$$\sum_{g=1}^{G}\left(\phi^{*g}, \frac{1}{v^g}\varphi^g\right) = constant \tag{5}$$

After some manipulation, the standard point reactor kinetics equations (PRKE) for the amplitude solution are obtained:

$$\frac{dp}{dt} = \left[\frac{\rho-\bar{\beta}}{\Lambda}\right]p + \sum_{i=1}^{I}\bar{\lambda}_i\xi_i \tag{6}$$

$$\frac{d\xi_i}{dt} = \frac{\bar{\beta}_i}{\Lambda} - \bar{\lambda}_i\xi_i \quad 1\le i\le I \tag{7}$$

Where the functional coefficients are calculated using the space-/time-dependent shape function as follows:

$$\frac{\rho-\bar{\beta}}{\Lambda} = \left[\sum_{g=1}^{G}\left(\phi^{*g}, \frac{\chi_p^g}{k_{eff}}(1-\beta)\sum_{g'=1}^{G}\nu^{g'}\Sigma_f^{g'}\varphi^{g'} + \sum_{g'\neq g}^{G}\Sigma_s^{g'\to g}\varphi^{g'} - \left(-\nabla\cdot D^g\nabla + \Sigma_r^g\right)\varphi^g\right)\right]\times\left[\sum_{g=1}^{G}\left(\phi^{*g}, \frac{1}{v^g}\varphi^g\right)\right]^{-1} \tag{8}$$

$$\frac{\bar{\beta}}{\Lambda} = \sum_{i=1}^{I}\frac{\bar{\beta}_i}{\Lambda} = \sum_{i=1}^{I}\frac{1}{k_{eff}}\frac{\sum_{g=1}^{G}(\phi^{*g},\chi_{d,i}^g\beta_i\sum_{g'=1}^{G}\nu^{g'}\Sigma_f^{g'}\varphi^{g'})}{\sum_{g=1}^{G}\left(\phi^{*g},\frac{1}{v^g}\varphi^g\right)} \tag{9}$$

$$\bar{\lambda}_i = \frac{\sum_{g=1}^{G}(\phi^{*g},\chi_{d,i}^g\lambda_i C_i)}{\sum_{g=1}^{G}(\phi^{*g},\chi_{d,i}^g C_i)} \tag{10}$$

IQS Predictor-Corrector (IQS P-C)

This version of IQS first solves the flux diffusion (represented by Equations 1 and 2) to get a predicted flux. The predicted flux at this step is then converted to shape by rescaling as follows:

$$\varphi^g_{n+1} = \underbrace{\phi^g_{n+1}}_{\text{predicted}} \frac{K_0}{K_{n+1}} \tag{11}$$

Where:

$$K_{n+1} = \sum_{g=1}^{G} \left(\phi^{*g}, \frac{1}{\nu^g} \phi^g_{n+1} \right) \tag{12}$$

$$K_0 = \sum_{g=1}^{G} \left(\phi^{*g}, \frac{1}{\nu^g} \varphi^g_{n+1} \right) = \sum_{g=1}^{G} \left(\phi^{*g}, \frac{1}{\nu^g} \phi^g_0 \right) \tag{13}$$

The PRKE parameters are then computed with this shape using Equations 8 - 10 and interpolated over the macro step, then the PRKE is evaluated. With the newly computed amplitude, the shape is rescaled and the corrected flux is evaluated:

$$\underbrace{\phi^g_{n+1}}_{\text{corrected}} = p_{n+1} \times \varphi^g_{n+1} \tag{14}$$

Time Adaptation

The time adaptation used for quantifying IQS's ability is step doubling. The step doubling technique involves estimating the local truncation error for a certain time step by taking the difference between a solution with one full step and a solution with two half steps. If the step is small enough, the error will be smaller than a user driven tolerance and the magnitude of the next step will be calculated based on the error. If the step is too large, the step will be repeated with a smaller step calculated with the resulting error. The error of the time step is approximated by Equation 15, where φ^g_1 and φ^g_2 are the solutions with the full step and half step, respectively. φ is changed to ϕ for regular flux evaluation and IQS P-C. If $e_n > e_{max}$ the time step is repeated; if $e_n < e_{max}$ the system moves to the next time step. The next Δt is calculated using Equation 16, where μ is the convergence order of the time integration scheme being used. e_{max} and e_{tol} are user defined parameters; e_{max} is usually less than e_{tol} to better guarantee that the calculated Δt_{new} will pass the error criteria so time steps won't be repeated.

$$e_n = \frac{\left\| \sum_{g=1}^{G} \varphi^g_2 - \sum_{g=1}^{G} \varphi^g_1 \right\|_{L^2}}{\max\left(\left\| \sum_{g=1}^{G} \varphi^g_2 \right\|_{L^2}, \left\| \sum_{g=1}^{G} \varphi^g_1 \right\|_{L^2} \right)} \tag{15}$$

$$\Delta t_{new} = \Delta t_{old} \left(\frac{e_{tol}}{e_n} \right)^{\frac{1}{\mu+1}} \tag{16}$$

To be clear, each solution is re-scaled by p when calculating e_n. Additionally, if the PJFNK iteration does not converge, the entire step doubling process is repeated with half the time original time step.

RESULTS AND ANALYSIS

This section describes results of an examples that tests the IQS implementation and shows its effectiveness on computation speed and accuracy. Two examples were selected for this purpose. The first is the two-dimensional TWIGL ramp transient benchmark, described further. The second is the LRA benchmark, which a two-dimensional, temperature feedback example. Each example was solved with regular diffusion (brute force) and IQS P-C. Each method was tested with backward-Euler for the TWIGL benchmark and Crank-Nicholson was used for the LRA benchmark. The performance for each method are represented by the number of macro time steps and solves with step doubling time adaptation.

TWIGL Benchmark

This benchmark problem originates from the Argonne National Lab Benchmark Problem Book [3]. It is a 2D, 2-group reactor core model with no reflector region shown in Figure 1. Table I shows the material properties of each fuel region and the ramp perturbation of Material 1.

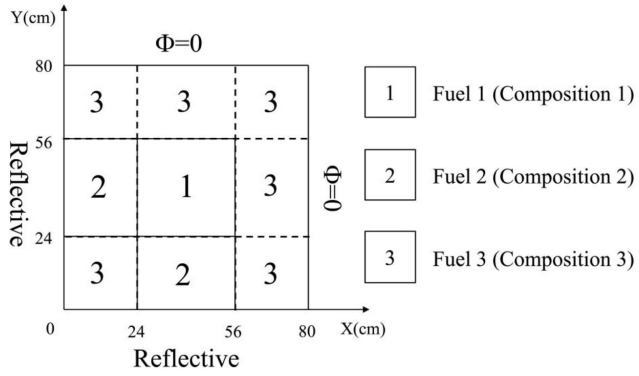

Fig. 1: TWIGL benchmark problem description

Material	Group	$D(cm)$	$\Sigma_a(cm^{-1})$	$\nu\Sigma_f(cm^{-1})$	χ	$\frac{\Sigma_s(cm^{-1})}{g \to 2}$
1	1	1.4	0.010	0.007	1.0	0.01
	2	0.4	0.150	0.200	0.0	0.00
2	1	1.4	0.010	0.007	1.0	0.01
	2	0.4	0.150	0.200	0.0	0.00
3	1	1.3	0.008	0.003	1.0	0.01
	2	0.5	0.050	0.060	0.0	0.00
	ν	$v_1(cm/s)$	$v_2(cm/s)$	β	$\lambda(1/s)$	
	2.43	1.0E7	2.0E5	0.0075	0.08	

Material 1 ramp perturbation:
$\Sigma_{a,2}(t) = \Sigma_{a,2}(0) \times (1 - 0.11667t) \quad t \leq 0.2s$
$\Sigma_{a,2}(t) = \Sigma_{a,2}(0) \times (0.97666t) \quad t > 0.2s$

TABLE I: TWIGL material properties and ramp perturbation

Figure 2 shows the IQS solution as compared with the Brute Force solution with minimal time steps. Table II shows the results for time adaptation. The results show that IQS performs exceptionally well compared to brute force for this highly transient example.

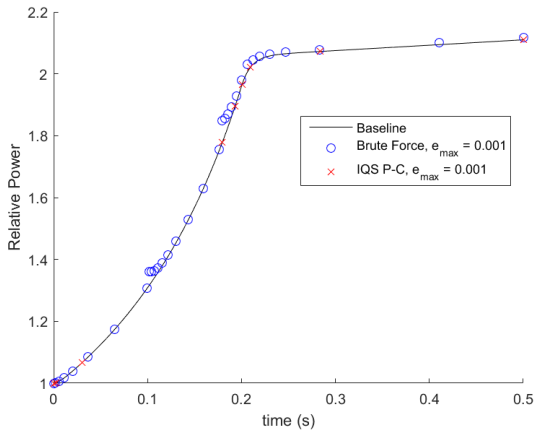

Fig. 2: Power level comarison of TWIGL benchmark between IQS and Brute Force using $e_{max} = 0.001$

		Brute Force			IQS P-C		
Test	e_{max}	Error	Steps	Solves	Error	Steps	Solves
1	0.05	0.00012677	9	29	0.03380433	4	9
2	0.01	3.5555e-05	5	40	0.00263068	5	12
3	0.005	4.0364e-05	5	40	0.00160486	6	21
4	0.001	0.00294822	5	36	1.7527e-05	10	35
5	0.0005	0.00099778	6	55	1.4185e-05	16	74
6	0.0001	0.00019510	7	65	6.2903e-06	19	78
7	5.0e-05	0.00018372	12	163	1.5247e-06	24	92
8	1.0e-05	8.0564e-05	379	5729	9.8321e-07	48	210

TABLE II: TWIGL step doubling results

LRA Benchmark

The LRA benchmark is a two-dimensional, two-group neutron diffusion problem with adiabatic heat-up and Doppler feedback in thermal reactor [3]. It is a super prompt-critical transient. To have better understanding on the cross sections given later, we present the equations here:

$$-\frac{1}{v_1}\frac{\partial \phi_1}{\partial t} = -\nabla D_1 \nabla \phi_1 + (\Sigma_{a,1} + \Sigma_{s,1\to 2})\phi_1 - \nu(1-\beta)S_f - \sum_{i=1}^{2}\lambda_i C_i, \tag{17}$$

$$-\frac{1}{v_2}\frac{\partial \phi_2}{\partial t} = -\nabla D_2 \nabla \phi_1 + \Sigma_{a,2}\phi_2 - \Sigma_{s,1\to 2}\phi_1, \tag{18}$$

$$S_f = \sum_{g=1}^{2}\Sigma_{f,g}\phi_g, \tag{19}$$

$$\frac{\partial C_i}{\partial t} = \nu\beta_i f - \lambda_i C_i, \quad i = 1,2, \tag{20}$$

$$\frac{\partial T}{\partial t} = \alpha f, \tag{21}$$

$$\Sigma_{a,1} = \Sigma_{a,1}(\boldsymbol{r}, t=0)\left[1 + \gamma\left(\sqrt{T} - \sqrt{T_0}\right)\right], \tag{22}$$

$$P = \kappa S_f, \tag{23}$$

where ϕ_1, ϕ_2 are the fast and thermal fluxes; v_1, v_2 are the averaged neutron velocities; $\Sigma_{a,1}, \Sigma_{a,2}$ are the absorption cross sections; $\Sigma_{s,1\to 2}$ is the fast-to-thermal scattering cross section; $\Sigma_{f,1}, \Sigma_{f,2}$ are the fission cross sections; ν is the averaged number of neutrons emitted per fission; β_1, β_2 are the delayed neutron precursor fractions and $\beta = \beta_1 + \beta_2$; C_1, C_2 are the delayed neutron precursor concentrations; λ_1, λ_2 are the decay constants of the delayed neutron precursors; $S_6 f$ is the fission reaction rate; P is the power density; T is the temperature; κ is the averaged power released per fission; α is the combination of κ and the specific heat capacity; γ is the Doppler feedback coefficient; $T_0 = T(\boldsymbol{r}, t=0)$. The two-group diffusion equation are solved with zero flux boundary conditions on external surfaces, reflecting conditions at symmetry boundaries and steady state initial conditions which are obtained by solving

$$-\nabla D_1 \nabla \phi_1 + (\Sigma_{a,1} + \Sigma_{s,1\to 2})\phi_1 = \frac{1}{k}\sum_{g=1}^{2}\nu\Sigma_{f,g}\phi_g, \tag{24}$$

$$-\nabla D_2 \nabla \phi_1 + \Sigma_{a,2}\phi_2 = \Sigma_{s,1\to 2}\phi_1 \tag{25}$$

The eigenvalue k is used to modify the fission cross section for the transient simulations with $\frac{1}{k}\Sigma_{f,g}, g = 1,2$. The initial flux distribution shall be normalized such that the averaged power density

$$\bar{P} \equiv \frac{\int_{V_{core}} P(\boldsymbol{r}, t=0)d\boldsymbol{r}}{\int_{V_{core}} d\boldsymbol{r}}, \tag{26}$$

where V_{core} is the core region with fuels, is equal to $10^{-6} W \cdot cm^{-3}$. The initial precursor concentrations are in equilibrium with the initial critical flux distribution.

The geometry is illustrated in Fig. 3.

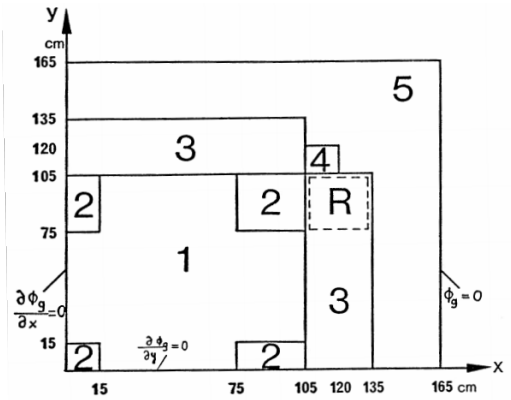

Fig. 3: LRA benchmark geometry with region assignment.

Initial two-group constants are presented in Table III. ν is equal to 2.43. Axial bulking $B^2 = 10^{-4}$ is applied for both energy groups. Delayed neutron data are presented in Table IV. All fuel materials have the same delayed neutron data. Some scalar data are listed in Table V.

The transient is initiated by changing the thermal absorption cross section as the following:

$$\Sigma_{a,2}(t) = \Sigma_{a,2}(t=0)\begin{cases} 1 - 0.0606184t, & t \le 2 \\ 0.8787631, & t > 2 \end{cases} \tag{27}$$

Region	Material	Group g	D_g (cm)	$\Sigma_{a,g}$ (cm^{-1})	$\nu\Sigma_{f,g}$ (cm^{-1})	$\Sigma_{s,1\to2}$ (cm^{-1})	χ_g	v_g ($cm \cdot s^{-1}$)
1	Fuel 1 with rod	1	1.255	0.008252	0.004602		1	3.0×10^7
		2	0.211	0.1003	0.1091	0.02533	0	3.0×10^5
2	Fuel 1 without rod	1	1.268	0.007181	0.004609		1	3.0×10^7
		2	0.1902	0.07047	0.08675	0.02767	0	3.0×10^5
3	Fuel 2 with rod	1	1.259	0.008002	0.004663		1	3.0×10^7
		2	0.2091	0.08344	0.1021	0.02617	0	3.0×10^5
4	Fuel 2 without rod	1	1.259	0.008002	0.004663		1	3.0×10^7
		2	0.2091	0.073324	0.1021	0.02617	0	3.0×10^5
5	Reflector	1	1.257	0.0006034	-		-	3.0×10^7
		2	0.1592	0.01911	-	0.04754	-	3.0×10^5

TABLE III: LRA benchmark initial two-group constants.

Group i	β_i	λ_i (s^{-1})	$\chi_{d,i,1}$	$\chi_{d,i,2}$
1	0.0054	0.0654	1	0
2	0.001087	1.35	1	0

TABLE IV: LRA benchmark delayed neutron data.

Meaning	Notation	value
Axial buckling for both energy groups	B_g^2	10^{-4} (cm^{-2})
Mean number of neutrons per fission	ν	2.43
Conversion factor	α	3.83×10^{-11} ($K \cdot cm^3$)
Feedback constant	γ	3.034×10^{-3} ($K^{1/2}$)
Energy released per fission	κ	3.204×10^{-11} ($J/fission$)
Initial and reference temperature	T_0	300 (K)
Active core volume	V_{core}	17550 (cm^2)

TABLE V: LRA benchmark scalar values.

where t is time in seconds.

Figure 4 shows the IQS P-C power profile as compared with the Brute Force solution. These plots show that IQS is consistent with Doppler feedback problems. Table VI shows the time adaptation performance of both methods. These results show that IQS, again, performs much better than the brute force method by taking significantly less time steps while retaining similar accuracy.

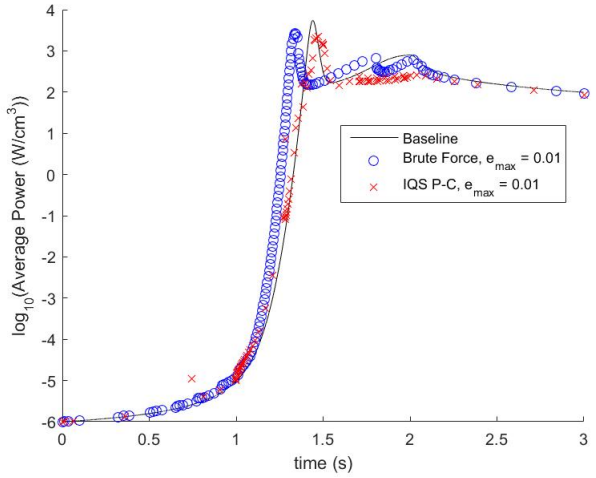

Fig. 4: Power level comarison of LRA benchmark between IQS and Brute Force using e_{max} = 0.01

		Brute Force			IQS P-C		
Test	e_{max}	Error	Steps	Solves	Error	Steps	Solves
1	0.01	3.5555e-05	145	735	0.00263068	105	616
2	0.005	4.0364e-05	266	948	0.00160486	157	814
3	0.001	0.00294822	585	2046	1.7527e-05	218	1062
4	0.0005	0.00099778	833	2908	1.4185e-05	480	2038
5	0.0001	0.00019510	1793	6155	6.2903e-06	434	1458
6	5.0e-05	0.00018372	2485	8511	1.5247e-06	542	1719

TABLE VI: LRA step doubling results

CONCLUSIONS

The purpose of this paper was to show IQS's performance with step doubling time adaptation. Two examples were used to quantify the method's performance, including the TWIGL and LRA benchmarks. The results from the TWIGL example shows significant improvement from the traditional brute force method. This improvement was anticipated because the shape for TWIGL changes very little through the transient, so the PRKE in IQS does most of the work. The results for the LRA benchmark showed similar improvement with less time steps for the same accuracy. In conclusion, IQS shows impressive performance for complex multi-physics problems with time adaptation. However, to rigorously test IQS, more complex problems including TREAT models and transport problems need to be applied.

ACKNOWLEDGMENTS

This work was supported by the Department of Energy and Idaho National Laboratory. Special thanks to Mark Dehart, NEAMS, and the Moose/Rattlesnake team at INL.

REFERENCES

1. K. OTT, "Quasi-static treatment of spatial phenomena in reactor dynamics," *Nuclear Science and Engineering*, **26**, 563 (1966).
2. S. DULLA, E. H. MUND, and P. RAVETTO, "The quasi-static method revisited," *Progress in Nuclear Energy*, **50**, *8*, 908 – 920 (2008).
3. P. BY THE BENCHMARK PROBLEM COMMITTEE OF THE MATHEMATICS and C. D. OF THE AMERICAN NUCLEAR SOCIETY, *Argonne Code Center: Benchmark Problem Book: Numerical Determination of the Space, Time, Angle, or Energy Distribution of Particles in an Assembly*, 3 ed. (1968).